Journal of Colloid and Interface Science 628 (2022) 684–695

Contents lists available at ScienceDirect

Journal of Colloid and Interface Science

journal homepage: www.elsevier.com/locate/jcis

Pectin-based microgels for rheological modification in the dilute to concentrated regimes

Samuel J. Stubley [a], Olivier J. Cayre [b], Brent S. Murray [a,*], Isabel Celigueta Torres [c]

[a] Food Colloids & Bioprocessing Group, School of Food Science & Nutrition, University of Leeds, LS2 9JT, UK
[b] Colloid and Polymer Engineering Group, School of Chemical & Process Engineering, University of Leeds, LS2 9JT, UK
[c] Nestlé Product Technology Centre, York, YO31 8FY, UK

GRAPHICAL ABSTRACT

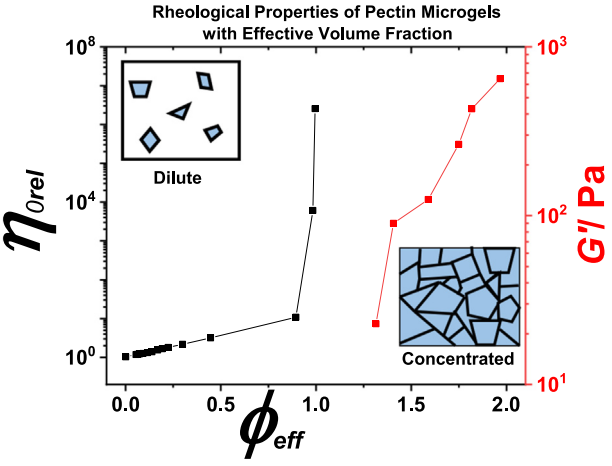

ARTICLE INFO

Article history:
Received 10 April 2022
Revised 14 June 2022
Accepted 23 July 2022
Available online 28 July 2022

Keywords:
Microgel
Gel
Sugar beet pectin
Viscoelasticity
Viscosity
Volume fraction
Laccase

ABSTRACT

Hypothesis: A novel range of microgel particles of different internal cross-linking densities can be created by covalently cross-linking sugar beet pectin (*SBP*) with the enzyme laccase and mechanically breaking down the subsequent parent hydrogels to sugar beet pectin microgels (*SBPMG*) via shearing. The bulk rheological properties of suspensions of the different *SBPMG* are expected to depend on the microgel morphology, elasticity (crosslinking density) and volume fraction respectively.

Experiments: The rheology of both dilute and concentrated dispersions of *SBPMG* were studied in detail via capillary viscometry and shear rheometry, supplemented by information on particle size and shape from static light scattering, confocal microscopy and electron microscopy.

Findings: For dilute suspensions of *SBPMG*, data for viscosity *versus* effective volume fraction (ϕ_{eff}) falls on a 'master' curve for all 3 types of *SBPMG*. In the more concentrated regime, the softer microgels allow greater packing and interpenetration and give lower viscosities at the same ϕ_{eff}, but all 3 types of microgel give much higher viscosities than the equivalent concentration of 'non-microgelled' pectin. The firmer microgels can be concentrated to achieve elasticities equivalent to the original parent hydrogel. All *SBPMG* suspensions were extremely shear thinning but showed virtually no time-dependence.

* Corresponding author.
E-mail address: b.s.murray@leeds.ac.uk (B.S. Murray).

https://doi.org/10.1016/j.jcis.2022.07.147
0021-9797/

1. Introduction

Microgel particles are solvent-swollen, particulate polymer networks spanning colloidal to millimeter dimensions. When prepared as suspensions, microgels have been proposed as novel additives to control the rheological properties of formulations of high solvent content, including pharmaceuticals, home and personal care products, agrochemicals and foodstuffs. The use of gels based upon polymer solutions introduces issues during processing due to the ease of which such gels can irreversibly rupture and fracture. In addition, storage stability may be affected due to molecular rearrangements post-processing, which in turn results in the exclusion of solvent from the gel network in a process known as syneresis [1]. In contrast, concentrated microgel suspensions are essentially 'solid-like' at rest but can be made to flow on the application of external forces that exceed an apparent yield stress [2], facilitating their 'processability' (e.g., pumping, molding, layering) and application (e.g., as topical pharmaceutical formulations or for appropriate oral sensations). This is potentially-one of the great advantages of microgel particles, which in principle can be fabricated from any gel-forming polymer. The rheology of such systems is mainly dictated by the (effective) volume fraction (ϕ_{eff}) occupied by the particles but also by the particle mechanical properties and particle–particle interactions [3].

The rheological properties of microgels composed of synthetic polymers have received significant interest in the scientific literature. Heterogeneous polymerization techniques are generally used to copolymerize monofunctional monomers with a suitable crosslinking monomer. Such 'bottom-up' techniques allow for great control over particle size and polydispersity. Synthetic protocols also allow for functionalization of the resulting polymer network for specific applications. For example, stimuli responsiveness, in terms of swelling or contraction due to temperature and/or pH changes, can be integrated through the selection of monomers such that the particle size (and thus ϕ_{eff}) can be controlled by changes in the environmental conditions [4]. Consequently, such systems have been used as model systems to study the physics of liquid–solid and solid–solid phase transitions, as reviewed extensively elsewhere [3,5,6].

In most cases, for microgels and 'model' hard spheres, polydispersity in particle size suppresses crystallization. Under these circumstances, the suspension is a disordered fluid until at $\phi \approx 0.58$, a so-called glass transition is observed. A glass refers to a dynamically arrested state of matter. Glassy behaviour persists to $\phi = 0.64$ (*i.e.,* the theoretical random close packing limit of equal sized spheres) although polydispersity and the presence of a 'soft' stabilizing layer at the particle surface for microgels and hard-sphere systems (i) complicates the definition of ϕ and (ii) pushes the ϕ required for phase transitions to higher values [7,8]. Soft particles such as microgels can be compressed and even interpenetrate at high phase volumes. Furthermore, their volume depends on the environmental conditions such as the osmotic pressure and, for stimuli responsive microgels, the solvent quality as noted above. Some authors discuss a jamming transition for colloidal hard spheres at $\phi > 0.64$, however this term is more frequently used to describe dense packings of non-colloidal particles, where Brownian motion is negligible and particles can be packed to such high ϕ that they form permanent contacts. The particle modulus and inter-particle friction then become important for the bulk rheological properties, particularly for the yielding behavior of these dense suspensions [2,3].

More recently, microgels based on biopolymers have emerged as attractive alternatives when taking into account both sustainability considerations and regulations for applications where biocompatibility is key. Biopolymer microgel particles have been fabricated using a variety of techniques (see reviews [9–11]). Notable examples are those prepared using the emulsion templating technique, whereby an aqueous biopolymer solution is emulsified into an immiscible fluid phase, followed by induction of gelation of the dispersed phase in some manner [12–14]. A disadvantage of this method is that microgel recovery from the immiscible continuous phase can be laborious due to the requirement for successive separation and washing steps, which can also damage their original templated geometry. Perhaps more scalable for industrial application is the preparation of so-called shear (fluid) gels, where the biopolymer solution is subjected to controlled shearing as gelation conditions are applied [15,16]. Under these conditions, gel network development is in competition with network break up due to the imposed flow, resulting in suspensions in which particle size and shape can be manipulated via the shear rate, polymer concentration and gelation kinetics [17]. An even more simple and scalable method to fabricate microgel suspensions is via the mechanical break-down of a pre-formed gel in the presence of excess solvent. The particle size and shape resulting from such 'top-down' techniques depend on the shear conditions and the mechanical properties of the original bulk 'parent' gel [18–21].

Pectin is an anionic heteropolysaccharide extracted from plant cell walls of agro-industrial waste streams. The pectin fine structure is complex and varies depending on the botanical origin and extraction conditions [22]. Generically, pectins demonstrate a block copolymer type structure with 3 main regions, namely homogalacturonan (*HG*), rhamnogalacturonan II (*RGII*) and rhamnogalacturonan I (*RGI*). The *HG* and *RGII* backbone is a linear polymer of 1,4-linked α-D-galacturonic acid (*GalA*) with the latter containing heteroglycan side chains [22,23]. The polymer backbone of RGI contains *GalA* with periodic rhamnose insertions. The rhamnose residues in this region bear neutral sugar side chains composed of arabinose and galactose [24]. In sugar beet pectin (*SBP*), ferulic acid residues are esterified to the neutral sugar side chains of *RGI* which can be deprotonated by oxidoreductase enzymes (e.g. laccases) [25] or chemical oxidizing agents (e.g. persulfates) [26]. The resulting phenoxyl radicals can subsequently react, resulting in covalent crosslinking of *SBP* molecules via ferulic acid dimers and/or higher ferulate oligomers [27]. Where the *SBP* concentration exceeds the polymer overlap concentration and there are sufficient ferulic acid residues available to form a percolated biopolymer network, such reactions lead to gelation. This phenomenon is the basis for the creation of the bulk *SBP* hydrogels that are subsequently sheared into smaller microgel particles in this work.

SBP microgels (*SBPMG*) prepared via this route demonstrate some interesting features which may provide significant advantages for commercial applications. For example, they are thermally stable, resist dissolution on extended storage in contact with aqueous solvents and appear to be robust to shearing - thus retaining their structural integrity under typical conditions experienced during processing and storage of consumer and industrial formulations [21]. In this paper, we describe in detail the bulk rheological properties of these novel *SBPMG*s, starting from an estimation of ϕ_{eff} for particles of different cross-linking density for both low and highly concentrated systems. The latter show remarkably high viscosities, reversible shear-thinning, plus some soft solid-like character at much lower concentrations of biopolymer than the native (*i.e.,* 'non-microgelled') *SBP* solutions. The *SBPMG* are therefore much closer to synthetic microgel systems, but are biocompatible and have great potential for rheological control and/or encapsulation.

2. Materials and Methods

2.1. Materials

Sugar beet pectin (GENU® Beta Pectin) (*SBP*) was a gift from CP Kelco (Lille Skensved, Denmark). Laccase Y120 (EC 1.10.3.2) was obtained from Amano Enzyme (Nagoya, Japan). Silicone oil with a viscosity of 350 cSt was obtained from VWR International (Paris, France). Type I (Milli-Q) water (Millipore, Bedford, UK) with a minimum resistivity of 18.2 MΩ cm was used throughout.

2.2. Fabrication of SBP hydrogels

SBP powder was dispersed into cold water using a T25 ULTRA-TURRAX rotor–stator mixing device equipped with an S25N – 18G dispersing tool (IKA, Oxford, UK) at 15,000 rpm. The powder was added gradually to prevent clumping and the resulting stock solutions were subsequently stirred magnetically for a minimum of 12 h in sealed Duran® bottles. *SBP* stock solutions at 3 different *SBP* concentrations (C_{PTOTAL}) were then centrifuged (Eppendorf 5810 R, Stevenage, UK) at 4000 rpm for 60 min in approximately 30 ml aliquots, to separate out any remaining insoluble material. The *SBP* solution supernatant was then carefully decanted and stored in sealed containers prior to further use. Separately, laccase stock solutions were prepared by solubilizing the enzyme powder in water for a minimum of 20 min.

For the generation of hydrogels, 25 ml of *SBP* stock solution and 5 ml of laccase stock solution were rapidly combined at ambient temperature by vortex mixing to give a final enzyme concentration of 0.1 mg ml^{-1} laccase, which was found to reproducibly give rise to homogeneous *SBP* gels. When the two solutions were visibly well mixed, hydrogels were allowed to develop quiescently in sealed containers for a minimum of 12 h by incubation at 25 °C. These hydrogels formed the 'parent' hydrogels used for the subsequent fabrication of microgel suspensions. Knowledge of the exact *SBP* concentration within bulk hydrogels (C_{GEL}) was required. In order to account for losses due to: potential incomplete solubilization of *SBP* powder, any insoluble material removed by centrifugation and any water associated with the powder before preparing the solutions, the gelation procedure outlined above was simulated by replacing enzyme solutions with water and drying the diluted *SBP* solutions in a vacuum oven (Townson and Mercer Limited, Croydon, England) at 75 °C and a pressure of 600 mm Hg until no change in mass was observed. This method was found to be more practical than attempting to dry bulk hydrogels. The same drying procedure was used throughout to determine C_{PTOTAL} in any microgel suspensions studied at a later date. The determination of C_{PTOTAL} allows for the calculation of an ϕ_{eff}, as described below.

2.3. Fabrication of SBP microgel suspensions

SBP microgel suspensions (*SBPMG*) were obtained from parent hydrogels prepared at C_{GEL} = 2.4, 3.4 and 4 wt% respectively. These were fabricated using the same ULTRA-TURRAX rotor–stator setup described above. The 'parent' hydrogels were firstly broken into coarse lumps with a metal spatula. Secondly, 25 g of these gel pieces were combined with 100 g of water (*i.e.,* suspensions were prepared at a nominal weight fraction of bulk gel to water of 20:80 wt%) prior to blending in the ULTRA-TURRAX at 10000 rpm for 10 min. Sodium azide (0.005 wt%) was added as a preservative after the fabrication of the microgel suspensions and to inhibit any further enzyme activity [28]. Although the hydrogels were allowed to develop quiescently for at least 12 h, we have previously shown [21] that gelation is almost complete after just 4 h (*i.e.,* there were no detectable changes in the G' after this time), presumably because all available ferulic acid residues had been consumed leaving no available sites for crosslinking within or between discrete microgel particles.

As explained above, C_{PTOTAL} for microgel suspensions was determined by drying + gravimetric analysis to account for any losses during sample preparation. C_{PTOTAL} can be converted to the concentration of *SBPMG* microgels (C_{SBPMG}) by [21]:

$$C_{SBPMG}(wt.\%) = 100 \times S \times \left(\frac{C_{PTOTAL}}{C_{GEL}}\right) \quad (1)$$

: accounting for C_{GEL} and the capacity for *SBP* gels (and thus microgels) to swell in the presence of excess solvent, pertinent due to the production technique used. The equilibrium swelling ratio, *S*, is already known from a previous study [21] and values for *S* are shown in Table 1. The lower degree of swelling for hydrogels prepared at higher C_{GEL} reflects an increased crosslinking density, since there are more ferulic acid residues present and these are the locus of crosslinking.

2.4. Particle size analysis of SBP microgel suspensions

Laser diffraction was performed to determine the particle size of *SBPMG*s prepared at different C_{GEL} via a Mastersizer 3000 equipped with the Hydro EV wet sample dispersion unit (Malvern Instruments, Worcestershire, UK). Suspensions were dispersed into pure water (20 °C) in the stirred measurement cell until the laser obscuration reached > 1 %. Particle size distributions (*PSD*) are inferred in the Mastersizer software from the angular dependence of scattered light intensity via the Mie theory for spherical particles. The Fraunhofer approximation gave good agreement in the calculated particle sizes. We are aware that *SBPMG* are not spherical and thus the *PSD*s are estimates, but complementary imaging suggested the apparent *PSD*s are reasonable (see Figure S1). Mean values of particle diameter, namely the Sauter (surface weighted) mean diameter ($D_{3,2}$) and the volume weighted mean diameter ($D_{4,3}$) are calculated according to:

$$D_{a,b} = \frac{\sum n_i D_i^a}{\sum n_i D_i^b} \quad (2)$$

where n_i is the number of particles of diameter D_i.

These are shown in Table 1. The *PSD*s were monomodal but naturally demonstrated some polydispersity.

2.5. Capillary viscometry of dilute SBP solutions and SBP microgel suspensions

Capillary viscometry was performed on dilute *SBP* solutions and also *SBPMG* suspensions in order to estimate ϕ_{eff}. An Ostwald-type U-tube viscometer was used (Reservoir size A, calibration constant, K = 0.003 mm^2/s^2) maintained at 20 ± 0.1 °C in a water bath. The efflux time was measured manually using a digital stopwatch with millisecond resolution. The relative (dynamic) viscosity (η_{rel}) is given by:

$$\eta_{rel} = \frac{\eta_s}{\eta_0} = \frac{K.t_0.\rho_s}{K.t_s.\rho_0} \quad (3)$$

where *t* is the efflux time, ρ is the density and the subscripts s and 0 refer to the suspensions/solutions and the pure solvent, respectively. Reported values for η_{rel} are based on the mean efflux times for a minimum of 3 measurements in the same viscometer.

Table 1
Elastic modulus (G'), loss factor (tanδ) and yield stress (σ_y) (defined as the shear stress σ at γ_y) measured in oscillatory shear rheology of 'parent' *SBP* hydrogels. The 'swelling ratio', S, was determined from equilibrium swelling experiments on the same hydrogels in a previous study [21]. Also shown are the surface weighted ($D_{3,2}$) and volume weighted ($D_{4,3}$) mean particle sizes of the resulting *SBPMG* suspensions determined via laser diffraction measurements.

C_{GEL} /wt.%	$G'_{\omega=0.01}$ /Pa	$G'_{\omega=100}$ /Pa	$\tan\delta_{\omega=0.01}$	$\tan\delta_{\omega=100}$	σ_y /Pa	S	$D_{3,2}$ /μm	$D_{4,3}$ /μm
2.4	118	110	0.010	0.293	33	1.50 ± 0.01	16.3 ± 0.1	32.0 ± 0
3.4	275	281	0.008	0.187	72	1.45 ± 0	37.0 ± 0.1	44.1 ± 0
4	712	662	0.011	0.150	126	1.42 ± 0.02	49.5 ± 0.2	57.9 ± 0.1

2.6. Shear rheometry of SBP hydrogels and SBPMG suspensions

An Anton Paar MCR 302 (Anton Paar GmbH, Graz, Austria) rheometer was used for all shear rheology experiments and the raw data were analyzed in the RheoCompass software. All rheological tests were performed using a 50 mm stainless steel parallel plate measuring set (PP50), with the gap set to 1 mm. The measurement geometry was covered by a custom-made circular plastic hood with dampened paper towel fixed to its inner circumference to prevent solvent evaporation in all cases. Unless stated otherwise, the measurement point duration was set to automatic using steady state sensing. Any rheological characterisation of *SBPMG* suspensions were performed using roughened plates, which were prepared by gluing water-resistant silicon carbide sandpaper (600 grit, from 3 M) to both the upper and lower plates *via* a multi-purpose silicone rubber sealant (Dow Corning 732), followed by curing for a minimum of 12 h before use. Roughened measuring sets were found to be important for preventing 'wall slip' for microgel samples in preliminary measurements. For characterisation of *SBP* hydrogels the original smooth plates were adequate.

All frequency sweep measurements were performed at strain amplitudes within the linear viscoelastic region (*LVER*) for the corresponding hydrogels or suspensions. The *LVER* was determined through trial and error during preliminary measurements not presented here. All strain amplitude sweeps were performed at an angular frequency of 6.28 rad s^{-1}. Strain (γ) amplitude sweeps on *SBP* hydrogels were carried out following the same protocol described above but using scaled down reaction volumes. The *SBP* + laccase solutions were rapidly mixed and immediately transferred to the rheometer gap. Following setting of the gap, hydrogels were allowed to develop quiescently at 25 °C for 2 h for C_{GEL} = 2.4 wt% or 4 h for C_{GEL} = 3.4 and 4 wt% respectively, the curing times selected based on the kinetics of gelation of these systems studied previously [21]. Due to the long experimental time, the edge of the sample was sealed with a high viscosity silicon oil (350 cSt) to provide additional protection against sample drying. Logarithmic strain sweeps with 8 data points per decade of γ, between γ = 0.01–100 % were employed. In separate experiments, frequency (ω) sweeps were also performed commencing after the specified setting times. Logarithmic frequency sweeps with 6 data points per decade between ω = 100 – 0.01 rad s^{-1} were employed.

For the rheological characterisation of the *SBPMG* suspensions prepared as described above, the samples were concentrated via mild centrifugation (4000 rpm, 60 min) to obtain a close packed pellet of *SBPMG*s followed by careful removal of the supernatant. The pellet was then diluted with a known amount of pure water and left at rest for 30 min (to allow for swelling/equilibration) in order to investigate the rheological properties in the concentrated regime over a range of ϕ_{eff}. This allowed us to prepare samples reproducibly while avoiding any complicating 'aging' effects which may arise from storing the samples in the concentrated regime. Furthermore, a 'shear rejuvenation' protocol was used prior to any measurements on the *SBPMG* suspensions: samples were pre-sheared at a shear rate of 50 s^{-1} for 30 s and left at rest for 15 min at 20 °C prior to commencing further experiments. Strain amplitude sweeps on *SBPMG* suspensions were performed in triplicate. Logarithmic strain sweeps were used with 8 data points per decade between γ = 0.01–100 %. For *SBPMG*s from: (a) C_{GEL} = 2.4 wt %, logarithmic frequency sweeps with 8 data points per decade between ω = 100 – 0.01 rad s^{-1} were employed, performed in duplicate; (b) C_{GEL} = 4 wt%, a single sample at ω = 100 – 0.1 rad s^{-1} was employed (*i.e.,* over a slightly reduced ω range to reduce the experiment time, since these suspensions were rather ω-independent at low ω).

For rotational tests on *SBPMG* suspensions (*i.e.,* viscosity measurements), logarithmic shear stress ramps were applied with 10 data points recorded per decade. Data points were recorded on reaching steady state or after a maximum of 5 min at each applied stress, whichever came first. Measurements were performed in triplicate using a new sample loading for each.

3. Results and discussion

3.1. Characterization of 'parent' SBP hydrogels

Fig. 1 shows the results of oscillatory shear rheometry experiments performed on hydrogels which were allowed to develop quiescently between parallel plates (*i.e., in situ*) due to the difficulty transferring pre-formed hydrogel discs to the rheometer. Over the range of C_{GEL} used (2.4, 3.4 and 4 wt%) the kinetics of crosslinking is mostly dictated by the enzyme (laccase) concentration [21] whilst the final storage modulus (G') is mainly controlled via C_{GEL}. Strain (γ) amplitude sweeps are shown in Fig. 1A for gels formed from the 3 different C_{GEL} at a fixed enzyme concentration (0.1 mg ml^{-1} laccase). All 3 gels showed a plateau in both G' and the loss modulus (G'') up until a strain amplitude of approximately 20 %, indicated by the vertical solid line and denoted as the 'yield strain' (γ_y), where deviations from the *LVER* were observed.

The length of the *LVER* therefore appears to be constant with respect to C_{GEL}, although the corresponding yield stresses (σ_y) differ. Indeed, it was found that for C_{GEL} = 4, 3.4 and 2.4 wt%, σ_y = 126, 72 and 33 Pa, respectively (see Table 1), *i.e.,* higher C_{GEL} led to higher moduli and σ_y, as expected. Comparison between the different systems is straightforward only within the *LVER*, but it is noted that all samples showed some evidence for strain hardening beyond γ_y. Thus, it is likely that the actual stresses required for gel fracture may be substantially higher than these values of σ_y. The sharp decline in G' at γ beyond the peak in G' and G'' illustrates the brittle fracture of the gels.

Fig. 1B shows data for frequency sweeps within the *LVER* (γ = 0.5 %). From a rheological standpoint, 'true' gel behavior can be defined as a frequency independent plateau in G' over an appreciable window in frequency (time), where $G' \gg G''$, *i.e.,* $\tan\delta = G''/G' <$ 0.1 say [29]. The values of tanδ at ω = 0.01 rad s^{-1} for all samples were < 0.1 and only increased slightly at ω = 100 rad s^{-1} (see Table 1) suggesting all 3 could be considered as gels. The increase in tanδ with ω is attributed to increased viscous dissipation due to network defects, for example any trapped sol fraction and dangling polymer chain ends [30,31].

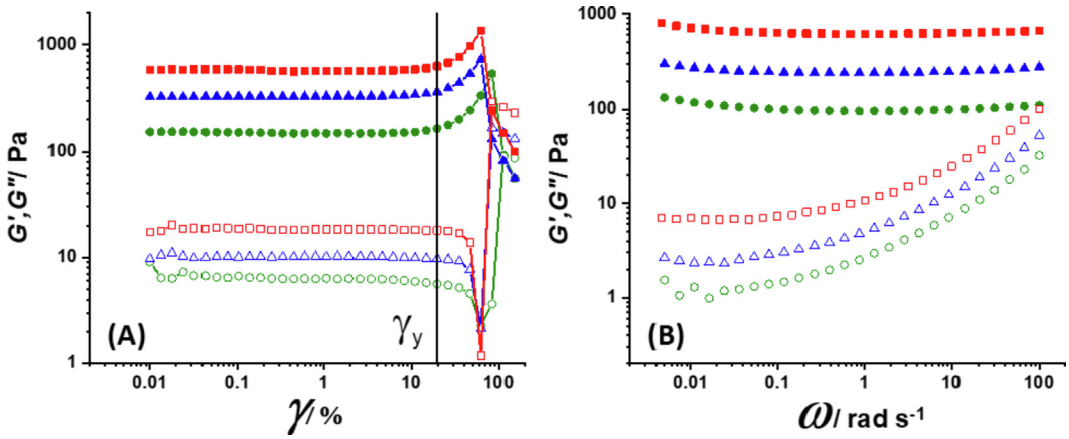

Fig. 1. Oscillatory shear rheometry performed on quiescently developed *SBP* hydrogels at C_{GEL} = 2.4 (●), 3.4 (▲) and 4 (■) wt.% *SBP* plus 0.1 mg ml^{-1} laccase. Closed symbols = *G'* and open symbols = *G''*. (A) Oscillatory strain amplitude sweeps at ω = 6.28 rad s^{-1}. Colored lines are to guide the eye. The vertical black line shows the apparent yield strain (γ_y) where *G'* deviates from linearity. (B) Oscillatory frequency sweeps at γ = 0.5 %. Experiments began 2 h (●) or 4 h (▲) and (■) after gap setting.

The surface weighted ($D_{3,2}$) and volume weighted ($D_{4,3}$) mean particle diameters of the *SBPMG*s produced via the mechanical disruption of the above gels are also given in Table 1. The volume weighted particle size distributions were reported previously [21]. It is seen that the gels with higher *G'* and σ_y gave rise to larger average *SBPMG* sizes. Similar findings have previously been reported for polysaccharide microgels prepared using a comparable 'top-down' approach, although these were gels based on agarose [19] and also low methoxyl pectins physically cross-linked with divalent cations [20].

In lieu of micromechanical characterization of individual microgel particles, it is usually assumed that the modulus of the microgel particles (referred to as G'_{MG} from hereon) is equal to that of a bulk gel prepared at the same polymer concentration [13,14]. This assumption has recently been shown to be reasonable for agarose microgel particles prepared using an emulsion templating technique with single particle properties then characterized via atomic force microscopy [12].

3.2. Rheology of dilute SBP microgel suspensions and estimation of ϕ_{eff}

The main objective for studying the rheological properties of dilute *SBPMG* suspensions was to determine ϕ_{eff}. However, from a technological perspective (*i.e.,* in industrial settings), determination of ϕ_{eff} is not necessarily required and C_{PTOTAL} is a more useful metric to use during formulation. In addition, the C_{PTOTAL} value is useful where ϕ_{eff} is estimated to exceed 1 as a result of the solvent content of the particles and their propensity for inter-penetration (see later). Using C_{PTOTAL} also allows for direct comparison of the microgel suspension properties to the corresponding *SBP* solutions. We will therefore consider the rheological properties of *SBP* microgel suspensions with respect to C_{PTOTAL} where appropriate. For example, Fig. 2 shows plots of reduced viscosity (η_{red}):

$$\eta_{red} = (\eta_{rel} - 1)/C \tag{4}$$

against C_{PTOTAL} for native *SBP* solutions (Fig. 2A) and for *SBP* microgel suspensions obtained from the 3 different parent gels (Fig. 2B). Extrapolation to C = 0 allows one to determine the intrinsic viscosity [η] according to:

$$[\eta] = \lim_{c \to 0}(\eta_{red}) \tag{5}$$

and the corresponding values from Fig. 2 are shown in Table 2, alongside the slopes of the curves. For the native *SBP* solutions, [η] was found to be 37.6 ± 2.4 dL g^{-1} , in agreement with previous studies [32,33]. Since microgel particles are cross-linked, supramolecular assemblies of *SBP* molecules, [η] is a measure of the specific volume of the particles (with units of volume/mass, dL g^{-1}).

It can be observed in Fig. 2B and Table 2 that [η] decreases with increasing C_{GEL} and therefore increasing *G'*, *G''* and σ_y (Table 1), *i.e.*, the 'softer' microgels demonstrated the highest [η]. The slope of these plots also follows the same order. Qualitatively, these findings suggest that with respect to C_{PTOTAL}, the softer microgels should be more effective at increasing the viscosity of the solvent with incremental addition of the dispersed material. This is to be expected, as suggested by Omari et al. (2006), who found [η] to range from 13.35 to 4.28 dL g^{-1} for colloidal Poly(*N*-isopropylacrylamide) *p(NIPAM)* microgels of varying crosslink density, the 'softest' microgels also demonstrating the highest values of [η]. The same authors also found that [η] for linear *p(NIPAM)* was higher (28.4 dL g^{-1}) than any of the microgels composed of the same polymer [34]. Shewan et al. (2015) obtained [η] = 12.8 dL g^{-1} for non-colloidal Carbopol suspensions, a commercially available poly acrylic acid microgel [13]. The [η] values reported in Table 2 for *SBPMG* therefore seem reasonable.

We note that for C_{GEL} = 3.4 wt% and C_{GEL} = 4 wt% the values of [η] were almost equal, within the experimental error (24.0 ± 2.6 and 20.3 ± 1.4 dL g^{-1} respectively) whilst for C_{GEL} = 2.4 wt% [η] was significantly larger (54.1 ± 1.1 dL g^{-1}). Considering the results of Omari et al. (2006), the increase in [η] suggests a tendency towards linear polymer behavior with increasing particle softness. However, [η] for the softest particles presented here was found to be greater even than for the non-gelled *SBP* solutions ([η] = 37.6 ± 2.4 dL g^{-1}). This finding suggests (i) the possible presence of some high *MW* aggregates, in effect microgel fragments, released from the softest gel in its conversion to *SBPMG* in addition to 'true' microgel particles or (ii) the presence of particle–particle interactions even at the apparently low particle concentrations used here, possibly due to the slightly hydrophobic nature of *SBP*, *i.e.*, producing hydrophobic patches in certain regions of the microgel 'surface'. Whatever the origin of this result, in practice it may be exploited to enhance the viscosity above that of simple solutions of *SBP* at the same C_{PTOTAL}.

Various complexities arise when interpreting the dilute suspension viscometry data, considering that the *SBPMG*s are *not* spherical (see Figure S1 for images of typical particle morphology). It is well known that the coefficient in the Einstein equation for [η] deviates from 2.5 for particle aspect ratios ≠ 1, due to particle orientation in flow [35] (which furthermore depends on Péclet number). Particle

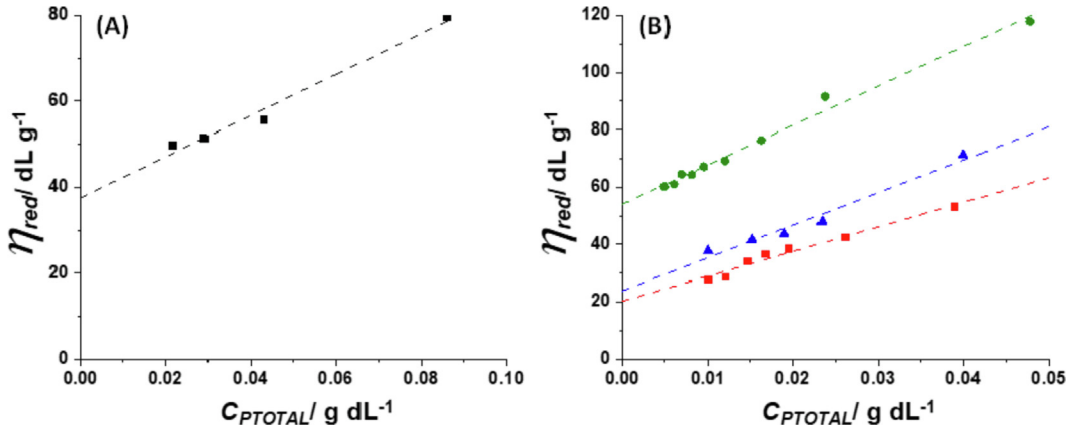

Fig. 2. Plots of reduced viscosity (η_{red}) as a function of C_{PTOTAL} for (A) dilute *SBP* solutions and (B) dilute microgel suspensions fabricated via the top-down mechanical disruption of bulk hydrogels at C_{GEL} = 2.4 (●), 3.4 (▲) and 4 (■) wt.%. Dashed lines are linear fits to the data. Extrapolation to C_{PTOTAL} = 0 gives the intrinsic viscosity [η] which is shown alongside the slope and coefficient of determination in Table 2.

Table 2
Intrinsic viscosity [η], slope and R^2 calculated from a linear fit to the data shown in Fig. 2. Also presented are the calculated values of k and R^2 obtained from fitting of the relative viscosity data shown in Fig. 3 to the modified Einstein (Eq. (6)) or modified Einstein-Batchelor (Eq. (7)) equations, respectively.

	Huggins			Einstein		Einstein-Batchelor	
Sample	[η]/ dL g^{-1}	Slope	R^2	k/ dL g^{-1}	R^2	k/ dL g^{-1}	R^2
2.4 wt% *SBPMG*	54.1 ± 1.1	1375 ± 56	0.989	0.04045 ± 5.7 × 10^{-4}	0.997	0.02939 ± 2.8 × 10^{-4}	0.996
3.4 wt% *SBPMG*	24.0 ± 2.6	1142 ± 110	0.973	0.03825 ± 1.1 × 10^{-3}	0.993	0.02739 ± 3.2 × 10^{-4}	0.996
4.0 wt% *SBPMG*	20.3 ± 1.4	862 ± 64	0.973	0.03224 ± 3.5 × 10^{-4}	0.997	0.02885 ± 3.1 × 10^{-4}	0.995
Native *SBP*	37.6 ± 2.4	478 ± 47	0.981	–	–	–	–

migration is also known to occur in the flow of non-Brownian suspensions through capillary channels [36]. Finally, soft *p(NIPAM)* microgels [37] and swollen starch granules [38] have been shown to change their morphology and volume in pressure driven and shear flows respectively, both of which can be experienced in capillary viscometers. While these issues may complicate the rheological analysis and ultimately lead to an overestimation of ϕ_{eff}, capillary viscometry was the best technique available to us to determine the rheological properties of suspensions in the dilute regime. Reassuringly, Fig. 3A shows that η_{rel} *versus* C_{SBPMG} (calculated according to Equation (1)) for all 3 types of *SBPMG* appear to fall on a master curve, indicating that any differences in particle modulus, or minor differences in shape, apparently have a negligible effect on the viscosity in the dilute regime.

The values of C_{SBPMG} can be converted to ϕ_{eff} by fitting η_{rel} data to both the modified Einstein (6) or modified Einstein-Batchelor (7) equations, respectively, which has become customary for microgel systems [13,39–41]:

$$\eta_{rel} = 1 + 2.5kC \tag{6}$$

$$\eta_{rel} = 1 + 2.5kC + 5.9kC^2 \tag{7}$$

where $C = C_{SBPMG}$ and k is a constant that subsequently allows for conversion of C to ϕ_{eff} via:

$$kC = \phi_{eff} \tag{8}$$

in the absence of inter-particle interactions and assuming spherical, monodisperse particles.

Fig. 3B and 3D shows the lines of best fit to Eq. (6) in the C_{SBPMG} range of 0–5 wt% and Fig. 3C in the range 0–7 wt%. Also shown in Fig. 3B to 3D are lines of best fit of Eq. (7) over the entire data set shown (*i.e.*, C_{SBPMG} up to 10 wt%). The corresponding fitted values of k are shown Table 2. It is seen that, not surprisingly, the modified Einstein-Batchelor equation (Eq. (7)) gives slightly better fits to the data when the higher C_{SBPMG} are included, with correspondingly lower k values. However, as a first approximation we have opted to use the k values from the modified Einstein equation (Eq. (6)) to estimate ϕ_{eff}, in view of the slight uncertainty in the quadratic term of Eq. (7) and the fact that *SBPMG* particles are not spherical or rigid and that other complications come to the fore when extrapolating these k values to more concentrated microgel dispersions – as discussed below. We simply note here that the k values are highest for the microgel particles formed from lowest C_{GEL} and we speculate that this means that the microgels formed from the softer gels probably have a more diffuse (or 'hairy') surface than those formed from the stronger gels. For example, other authors [41] have noted higher k values for less densely crosslinked *p(NIPAM)* microgels, which are expected to have a more diffuse interfacial region.

3.3. Rotational shear rheometry of concentrated SBPMG suspensions

Typical steady state viscosity (η) curves for microgel suspensions prepared from C_{GEL} = 2.4 wt% are shown as a function of shear stress (σ) in Fig. 4A and as a function of shear rate ($\dot{\gamma}$) in Fig. 4B. Repeat

measurements were performed using the rheometer in a stress-controlled mode of operation and $\dot{\gamma}$ was calculated according to $\dot{\gamma} = \sigma/\eta$, thus introducing error in the x-direction for the $\eta(\dot{\gamma})$ curves. The corresponding viscosity curves for *SBPMG* samples prepared

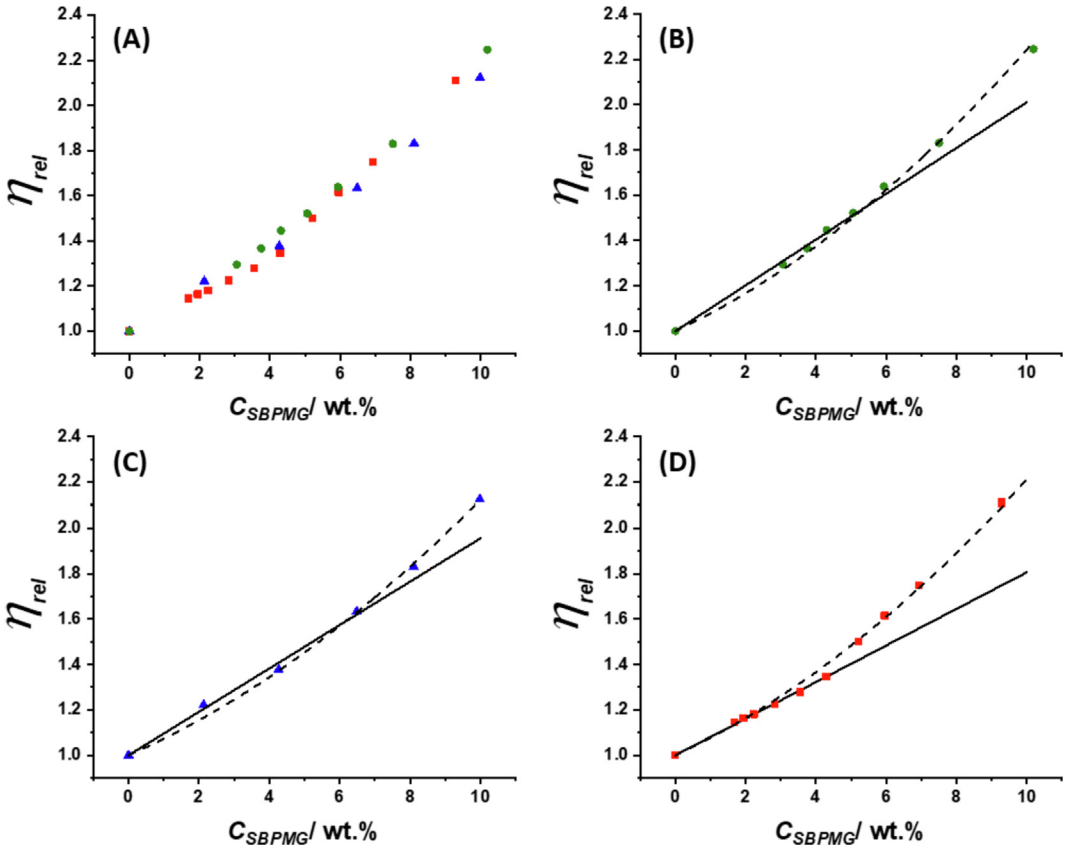

Fig. 3. Relative viscosity (η_{rel}) as a function of microgel particle concentration (C_{SBPMG}) for dilute *SBP* microgel suspensions. Eq. (1) was used to convert C_{PTOTAL} to C_{SBPMG}. (A) All microgel samples prepared from their parent hydrogels C_{GEL} = 2.4 (●), 3.4 (▲) and 4 (■) wt.%. (B-D) Curve fitting to microgel suspensions according to the modified Einstein equation (Eq. (6), solid lines) or the modified Einstein-Batchelor equation (Eq. (7), dashed lines) for *SBPMG* samples prepared at: (B) C_{GEL} = 2.4 wt%; (C) C_{GEL} = 3.4 wt%; (D) C_{GEL} = 4 wt%. Calculated values of k and R^2 are given in Table 2.

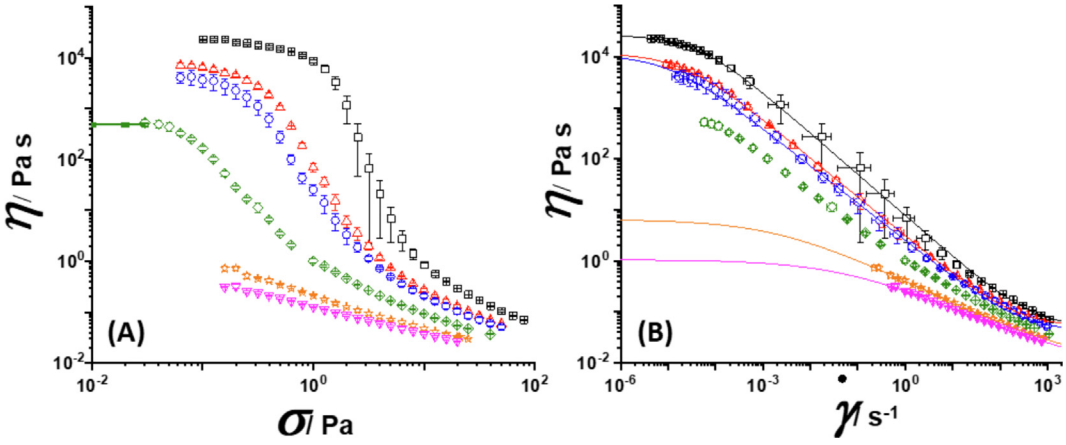

Fig. 4. Steady state viscosity (η) curves for concentrated *SBPMG* suspensions (C_{GEL} = 2.4 wt%) presented as a function of (A) shear stress (σ) and (B) shear rate ($\dot{\gamma}$). ϕ_{eff} for these samples were ■=2, ▲=1.85, ●=1.77, ◆=1.57, ★= 1.54 and ▼=1.42. Solid lines in 4B are fits to the Cross model (Eq. (9)). Calculated parameters are shown in Table 3. The solid line in 4A shows the average η and standard deviation for the first three data points (*i.e.*, data within the pseudo Newtonian plateau). This allows an estimation of the 'zero shear' η where the Cross model cannot be fit to the data.

from C_{GEL} = 3.4 wt% and C_{GEL} = 4 wt% are shown in Figure S2. In most cases, a low shear Newtonian plateau (hereafter referred to as the 'zero shear' viscosity, η_0) is observed where η is essentially independent of σ. This is thought to correspond to creeping flow before a critical σ is reached, at which point the suspensions appear to yield strongly as characterised by a decrease in η by several orders of magnitude over a narrow range of σ. This steep reduction in η has previously been suggested as a hallmark of yield stress fluids [42]. However, one may argue that if suspensions flow with a constant η at low σ then a yield stress is, by definition, absent. Indeed, when η is plotted as a function of $\dot{\gamma}$, the corresponding reduction in η appears more gradual. Pseudoplasticity was observed in all cases and η_0 of the order of 10^4 –10^5 Pa s can be achieved depending on ϕ_{eff} and G'_{MG}. Only in the softest microgel suspensions (Fig. 4A and 4B) is there evidence for the approach to a high shear rate limiting Newtonian plateau (hereafter referred

to as the 'infinite shear viscosity' (η_∞)). The η of firmer microgel suspensions appears to continuously decrease with further increases in σ or $\dot{\gamma}$ (Figure S2). The upper σ investigated corresponds to $\dot{\gamma} \approx 1000\ s^{-1}$ in all cases, which seemed to be the maximum accessible $\dot{\gamma}$ before the samples were ejected from the gap between the parallel plate measuring set. Consequently, only the softest microgel samples could be described by the Cross model [43] (Eq. (9)) with the exception of the sample prepared at ϕ_{eff} = 1.57 (Fig. 4B):

$$\eta = \eta_\infty + \frac{\eta_0 - \eta_\infty}{1 + (K\dot{\gamma})^m} \quad (9)$$

where m is the shear thinning exponent and K is the 'consistency' index. This model has previously been used to describe the pseudoplasticity observed in viscosity curves of microgel suspensions [15,41,44]. The fitting parameters are shown in Table 3.

The shear thinning exponent, m is found to decrease with a reduction in ϕ_{eff} whereas no trend was found in the consistence index, K. The η_0 for all other samples were estimated from the η (σ) plots by averaging the first 3 data points. The η_∞ were estimated from the $\eta(\dot{\gamma})$ plots using a linear fit to the high shear data in the range $\dot{\gamma} \approx$100-800 s^{-1} and interpolation of η to a value at $\dot{\gamma}$ = 500 s^{-1}. Estimates of η_0 and η_∞ (Table 3) will be used for a further analysis of the rheological properties of the suspensions described below. The corresponding values of η_0 and η_∞ extracted from the flow curves for C_{GEL} = 3.4 wt% and C_{GEL} = 4 wt% shown in Figure S2 are given in Table S1. The range of ϕ_{eff} apparently tested here was high (ϕ_{eff} > 1 in most cases) (Fig. 4 and Figure S2). For monodisperse hard spheres, the theoretical maximum random packing fraction, ϕ_{max}, is estimated as ϕ = 0.64. The non-spherical nature, compressibility and polydispersity [21] of particles can all increase ϕ_{max} [45,46] as discussed in the Introduction and here ϕ_{eff} was estimated by extrapolation from values determined at 'infinite' dilution. The calculated values of k used to convert C_{SBPMG} to ϕ_{eff} (Eq. (6)) do not account for the possibility of osmotic deswelling [44,47] or the potential for deformation and interpenetration of soft particles as ϕ_{eff} increases [5], leading to overestimates in ϕ_{eff}. For these reasons, apparent ϕ_{eff} > 1 are regularly reported for microgel systems [34,40,41,48,49]. The degree of osmotic deswelling is difficult to observe or measure directly and at a fixed ϕ, de-swelling depends upon a number of different factors including the micromechanical properties of the particles, the change in concentration of ions within and outside the particles as the system is concentrated, plus the other solvent conditions. Nonetheless, when we investigate the dependence of ϕ_{eff} on the *relative* 'zero shear' (η_{0rel}) (Fig. 5A) and *relative* 'infinite' shear ($\eta_{\infty rel}$) viscosities (Fig. 5B) we can observe distinct differences between samples which we therefore assume to be dependent only on G'_{MG}.

Fig. 5A is constructed from the η_{rel} data determined by capillary viscometry on the dilute suspensions and shear rheometry on more concentrated samples. The increase in η_{0rel} with ϕ_{eff} is initially gradual for all samples before increasing dramatically over a narrow range in ϕ_{eff} which is typical of particle suspensions. According to the Krieger-Dougherty relation [50], the divergence of η_{0rel} occurs at $\phi_{max,}$ which clearly occurs at relatively higher ϕ_{eff} for the softer particles. The suspensions can apparently be concentrated further, reflecting the potential for particles to de-swell, interpenetrate and deform, as discussed above. This is evident from the data points recorded beyond the region of divergence where the increase in η_{rel} becomes more linear, resulting in an 'S-shaped' curve (and is even more apparent when plotted on a log-linear plot as in Figure S3). Samples prepared at even higher ϕ_{eff} were studied by oscillatory rheometry and are discussed in the next section.

Shear thickening, *i.e.*, the increase in η with increasing $\dot{\gamma}$ or σ, is a well-known phenomenon in hard sphere systems and can introduce significant challenges during processing (e.g. spraying, coating, mass transport) of suspensions with a high solid content. Fig. 4 and Figure S2 suggest that shear thickening is absent in *SBPMG* suspensions over the range of ϕ_{eff} and σ investigated here. Fig. 5B shows that the relative high shear viscosity of *SBPMG*s appears to increase more gradually with ϕ_{eff} and this is typical of soft particle suspensions [14,41,51]. In addition, there appears to be an effect of G'_{MG} on the high shear viscosity data, with the firmest microgels demonstrating the highest $\eta_{\infty rel}$ at equivalent ϕ_{eff}. This agrees with the limited number of similar studies and has been attributed to the deformability of the particles, which consequently leads to differences in the particle packing efficiency [14,15]. Due to the high $\dot{\gamma}$ investigated, one cannot rule out the possibility for solvent (water) to be 'squeezed' out of discrete particles during these measurements which would lead to a reduction in ϕ_{eff} and thus η_{rel} [38]. The exponents of power law fits in Fig. 5B are greatest for the softest particles and are higher than those previously reported for κ-carrageenan fluid gels [15].

3.4. Oscillatory shear rheometry of concentrated SBPMG suspensions.

Fig. 6A and 6B show typical frequency sweep data for a series of *SBPMG* suspensions prepared from C_{GEL} = 2.4 wt% and C_{GEL} = 4 wt% respectively (*i.e.*, the softest and most firm microgels, respectively). It can be observed that G' is essentially independent of frequency and $G' > G''$ over a considerable frequency range, indicating solid-like behavior for all samples studied, as expected of concentrated suspensions.

The elasticity presumably arises from particle-particle contacts that produce an interconnected microstructure [2,14]. This is

Table 3
Fitting parameters calculated from fitting the Cross model (Equation (9)) to the data shown in Fig. 4B. Also shown are the interpolated values of η at $\dot{\gamma}$ = 500 s^{-1}, which are used to compare relative high shear viscosity data for all *SBPMG* samples shown in Fig. 5B. For the sample prepared at ϕ_{eff} = 1.57, the Cross model cannot be used and η_0 was estimated from the $\eta(\sigma)$ plots with the average and standard deviation calculated using the first three data points (*i.e.*, data within the pseudo Newtonian plateau) as shown in Fig. 4A.

ϕ_{eff}	η_0 (Pa s)	η_∞ (Pa s)	K (Pa s)	m	η at $\dot{\gamma}$ = 500 s^{-1} (interpolated)
2	26,959 ± 1215	0.049 ± 0.025	23,872 ± 3973	0.809 ± 0.007	0.201 ± 0.003
1.85	11,912 ± 1039	0.051 ± 0.003	48,886 ± 6989	0.765 ± 0.031	0.105 ± 0.008
1.77	11,225 ± 3733	0.041 ± 0.002	94,416 ± 55,466	0.734 ± 0.010	0.102 ± 0.009
1.57	467 ± 34	–	–	–	0.901 ± 0.001
1.54	6.5 ± 2.55	0.0020 ± 0.0005	459 ± 469	0.448 ± 0.008	0.602 ± 0.002
1.42	1.1 ± 0.20	0.0077 ± 0.0015	0.423 ± 0.017	0.424 ± 0.017	0.052 ± 0.002

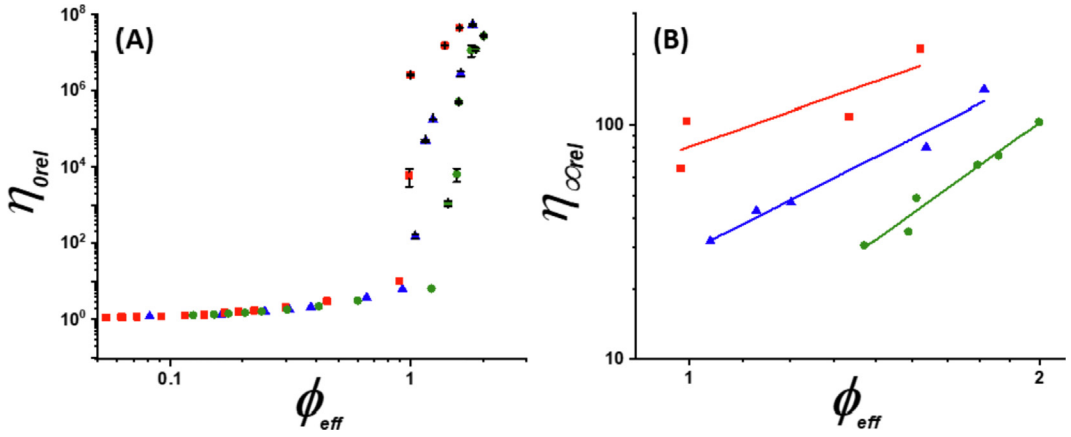

Fig. 5. (A) Relative 'zero shear' viscosity (η_{0rel}) and (B) relative 'infinite shear' viscosity ($\eta_{\infty rel}$) as a function of ϕ_{eff} for *SBPMG* suspensions shown on a double logarithmic plot. *SBPMG* suspensions were prepared at C_{GEL} = 2.4 (●), 3.4 (▲) and 4 (■) wt.%. In (B), data are fitted to a power law model and the corresponding power law exponents were 4.2 ± 0.4, 3.3 ± 0.2 and 2.1 ± 0.9 respectively.

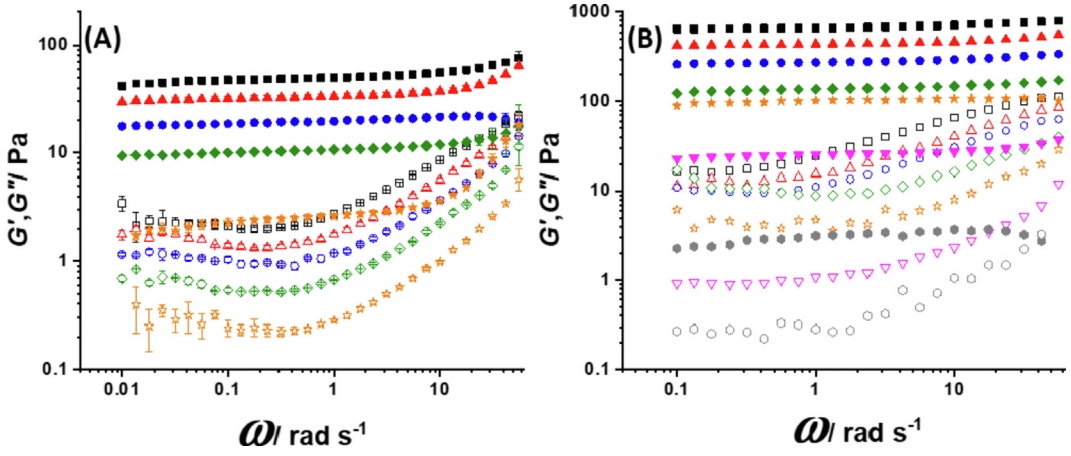

Fig. 6. Frequency sweeps performed at strain amplitudes within the *LVER* on *SBPMG* suspensions prepared over a range of ϕ_{eff} for (A) C_{GEL} = 2.4 wt% and (B) C_{GEL} = 4 wt%. Closed symbols = *G'* and open symbols = *G"*. In (A), ϕ_{eff} for these samples were: ■=2.35, ▲=2.22, ●=2.02, ◆=1.9 and ★=1.44. In (B), ϕ_{eff} for these samples were: ■=1.97, ▲= 1.82, ●=1.75, ◆=1.59, ★=1.41, ▼=1.32 and ⬢= 1.24.

typical where ϕ_{eff} exceeds the value of close packing or in the presence of some fractal-type particle aggregates which span the entire system, as in particle gels [52]. Note that here ϕ_{eff} > 1, so that certainly the former is probably the case. One might expect to find a viscoelastic fluid region (*G"* > *G'*) before the onset of elasticity, as observed previously for a variety of hard sphere [52,53] and soft particle [12,14,41,54–57] suspensions. However, resolving the viscoelastic moduli of samples more dilute than those shown here proved challenging with the instrument available: experimental data were not very reproducible. The variation of *G"* with frequency is more complex and demonstrates a minimum at intermediate frequencies that is more apparent for the softer microgel particles shown in Fig. 6A. This minimum in *G"* appears to become more pronounced with increasing dilution, as found in concentrated emulsions [55]. Also, this behavior has been observed for other soft particle suspensions at ϕ beyond the glass transition [54,56–58], perhaps providing further evidence that the samples studied here are 'jammed' systems and not particle gels possessing a true yield stress.

Fig. 7 shows the strong dependence of *G'* on ϕ_{eff} for these samples and captures the influence of particle modulus (G'_{MG}) on the bulk rheological properties, *G'* reaching higher values for the most firm microgels. From the linear fits (gradient n) to the plots of $\log_{10}$G' *versus* $\log_{10}\phi_{eff}$, it is clear that *G'* of the firmer microgel particles increases more strongly (n = 7.6 ± 0.9) with ϕ_{eff} than those prepared with softer microgels (n = 6.2 ± 0.3). Other studies have reported similar exponents [2,14,49,54] suggesting some universality between the rheological properties of soft particle suspensions in the concentrated regime, irrespective of particle type, size or morphology. For example, exponents ranging from 3.19 to 8.3 have been reported for *p(NIPAM)* microgel particles, exponents increasing with crosslinking density and thus particle modulus [41,48]. Exponents of 7 and 7.7 were found for κ-carrageenan fluid gels [15] and swollen poly(methyl methacrylate) (PMMA) spheres [59] respectively.

The above behavior is in contrast to hard spheres, for which *G'* has been reported to demonstrate a much stronger dependence on ϕ depending on the range of ϕ investigated. For example, van der Vaart et al. (2013) showed that *G'* for dense PMMA spheres diverged in the vicinity of ϕ_{max} in a similar fashion to the viscosity (*i.e.,* according to the Krieger-Dougherty relation) [40] whereas Koumakis et al. (2012) found exponents ranging from 30 at ≈0.54 > ϕ < 0.6 and 50 at ϕ > 0.6. Meanwhile, 'ultra-soft' colloidal suspensions such as star-like polymer micelle glasses were found [54] to demonstrate exponents of around 2. A theoretical study on the rheology of multi- arm star polymers predicts a linear increase above ϕ_{max} [60]. Thus, the *SBPMG* and other microgel particles behave as intermediate between hard spheres and ultra-soft

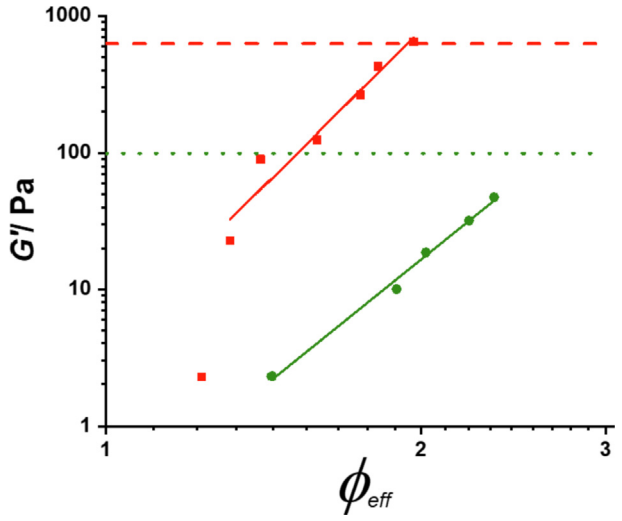

Fig. 7. Storage modulus (G') of *SBPMG* suspensions (C_{GEL} = 2.4 (●) and 4 (■) wt.%) as a function of ϕ_{eff}. Data points are taken from frequency sweeps shown in Fig. 6 at ω = 0.1 rad s^{-1} and at 20 °C. The solid lines show a power law fit to the data (neglecting the first data point in samples prepared at C_{GEL} = 4 wt%). The power law exponents were ● = 6.2 ± 0.3 and ■ = 7.6 ± 0.9. The horizontal dashed lines show the G' of "parent" hydrogels at ω = 0.1 rad s^{-1} for C_{GEL} = 2.4 wt% (green dotted line) and 4 wt% (red dashed line) at 25 °C.

colloidal systems. The definition of the latter system could be extended to include polymer coils in solution, which are currently more widely used for rheology modification [61].

The horizontal lines in Fig. 7 show G' of the respective 'parent' hydrogels at 25 °C. The suspensions were studied at a slightly lower temperature of 20 °C, but despite this caveat, it can be observed that G' of the suspensions closely approaches that of the parent hydrogels at the highest ϕ_{eff} investigated. Interestingly, this occurs at substantially lower values of C_{PTOTAL} for the suspensions, again showing how processing can be made more economical when *SBP* hydrogels are converted to microgel suspensions in order to impart solid-like rheological properties to a given formulation. For example, the corresponding C_{PTOTAL} for the firm microgels (C_{GEL} = 4 wt%) at ϕ_{eff} = 1.97 was 1.72 wt%. The highest C_{PTOTAL} investigated for the microgels prepared at C_{GEL} = 2.4 wt% was 0.93 wt%. The microgel samples evidently display significant elasticity even at low overall C_{PTOTAL}. In contrast, elasticity in linear polymer solutions generally arises at high polymer concentrations and on timescales shorter than the relaxation time, since it originates from chain entanglements [1,34].

van der Vaart et al. (2013) showed that G' for dense p(NIPAM) microgel suspensions was around an order of magnitude lower than the Young's modulus (E_P = 5.2 kPa) of the discrete *p(NIPAM)* microgel particles (as measured by atomic force microscopy (AFM)) [40]. The *p(NIPAM)* microgels were significantly firmer than those presented in our study, assuming that $G'_{MG} = G'$ of the corresponding hydrogel, so that our *SBPMG* probably have a greater capacity for interpenetration and 'merging together' to reform a structure similar to the parent hydrogel.

Shewan et al. (2021) analyzed their $G'(\phi)$ data for emulsion templated agarose microgel suspensions [12] with the model of Evans and Lips [62], which is based on the theory of Hertzian contact mechanics and incorporates the elastic modulus of microgel particles. The use of the Young's (compressive) modulus measured by AFM was found to give a better fit to the data compared to the use of a particle shear modulus (*i.e.*, G'_{MG}), estimated from the G' of a hydrogel prepared at the same polymer concentration. However, in neither case did G' of the dense suspensions reach the measured or estimated G' of the particles, which again were substantially firmer than those presented here.

These comparisons perhaps emphasize further the potential advantages of using *SBPMG* or similar microgels as rheology modifiers and show how the mechanical properties of formulations could be tailored simply by incorporating combinations of particles which differ in their material properties.

Fig. 8 shows the results of strain amplitude (γ) sweeps performed on *SBPMG* suspensions over a wide range in ϕ_{eff}. The G' data has been scaled as G'/G'_0 where $G'_0 = G'$ in the *LVER*. This analysis shows deviations from the *LVER* more clearly when data for several samples are plotted on the same Figure. The viscous modulus is evaluated through tanδ, that is, tanδ = G''/G'. The variation of G' and G'' with γ, showing absolute values of the viscoelastic moduli, are shown in supplementary Figure S4 and are in good agreement with the frequency sweep data presented in Fig. 6 and discussed above.

The data shows that with decreasing ϕ_{eff}, the plateau modulus (see Figure S4) and length of the *LVER* (Fig. 8A and 8B) are reduced for both samples studied, implying a concurrent reduction in the number and strength of inter-particle interactions with increasing dilution. Such interactions will include entanglements of the 'fuzzy' surface of such particles and any weak non-covalent forces operating between the constituent sugars of the polysaccharide chains. The value of tanδ increases with γ from < 1 to values > 1 at the γ tested, suggesting that the initially solid-like samples yield and begin to flow as a viscoelastic fluid [40,63], since this corresponds to the condition where $G'' > G'$. Similarly, the maximum in G'' observed before this crossover (Figure S4) has previously been associated with the dissipation of energy on yielding of colloidal gels [53] and glasses [49,54]. Repeat measurements were performed on the same sample using the rejuvenation protocols described in the Methods section prior to starting each measurement. The error between measurements was very small, suggesting that the particle material properties were largely unchanged after exposing the suspensions to high γ. The solid–fluid transition must therefore be attributed to deformation of the suspension microstructure with respect to the location and orientation of discrete particles [64,65]. However, the *SBPMG* particles appear to assume a close packed microstructure following shear rejuvenation (*i.e.*, on the cessation of shear after an appropriate time at rest) since the plateau modulus was recovered on repeating the measurement. The γ where deviations from the *LVER* occur (Fig. 8) could be taken as a measure of the critical strain (γ_c) for yielding. Other authors have noted increases in γ_c as a function of ϕ for soft particle suspensions [54,63,66]. However it should be noted that Ketz et al. (1988) found dense Carbopol suspensions (polyacrylic acid microgels) to yield at a constant γ_c, independent of particle concentration (ϕ) [67].

The G' of *SBPMG* samples prepared at C_{GEL} = 4 wt% and ϕ_{eff} = 1.24 (Fig. 8B and Figure S4B) is relatively low ($G' \approx 5.7$ Pa at γ = 0.01 %) and appears to drop off more strongly and at substantially lower γ_c ($\gamma_c \approx 0.1$ %) than any other samples tested, for both firm and soft microgels (Figures 8 and S4). This may suggest that these particles are in contact but not yet interpenetrating despite the high apparent ϕ_{eff} (ϕ_{eff} = 1.24). One might expect that microgels formed from the stronger gels would have a less 'fuzzy' and open surface, either due to their inherently higher cross-linking density or the way this cross-linked structure survives on fragmentation to microgels under shear. At present, however, we do not have microscopy tools of sufficient resolution to prove this by direct observation. The G' appeared to reach a minimum at $\gamma \approx 10$ % before increasing again as γ increased. Similar behavior was observed in other more dilute samples over the γ range studied. Such behavior may be attributed to wall slip at high γ [53], despite the use of roughened measuring sets and the reproducibility of the measurements. Another possibility for the increase in G' at high γ is due to shear thickening, as found in hard sphere glasses [68] although this was not

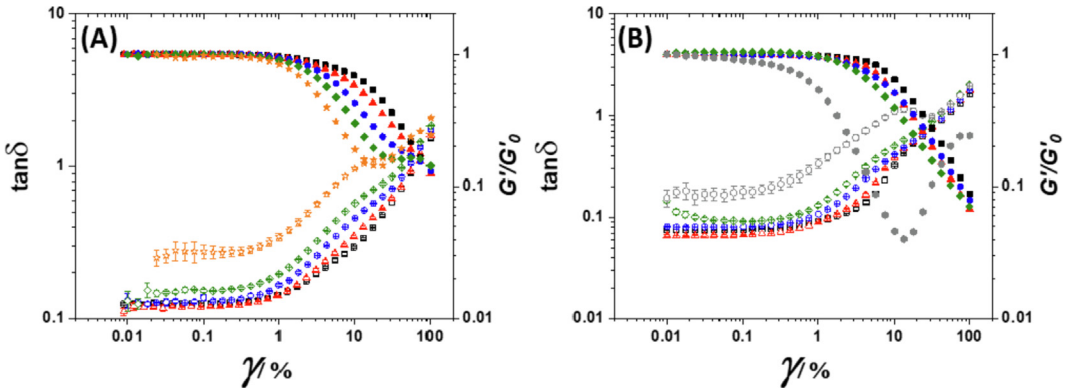

Fig. 8. Oscillatory strain amplitude (γ) sweeps for *SBPMGs* over a range in ϕ_{eff} for (A) C_{GEL} = 2.4 wt% and (B) C_{GEL} = 4 wt%. On the right-hand side y-axis of both (A) and (B), experimental G' was normalized by G' in the *LVER* (G'_0). Closed symbols = G'/G'_0. On the left-hand side y-axis of both (A) and (B), the variation of tanδ (*i.e.* G''/G') with γ is also plotted. Open symbols = tanδ. In (A), ϕ_{eff} for these samples were: ■=2.35, ▲=2.22, ●=2.02, ◆=1.9 and ★=1.44. In (B), ϕ_{eff} for these samples were: ■=1.97, ▲=1.82, ●=1.75, ◆=1.59, ★=1.41, ▼=1.32 and ⬢ = 1.24.

observed in any of our steady state viscosity measurements performed at lower ϕ_{eff}. Taking γ even higher may reveal the same behavior in the most concentrated samples and requires further investigation.

4. Conclusions

Building on previous work [21] showing that it is possible to create a range of robust microgel particles from *SBP* via laccase catalyzed crosslinking, we have addressed our hypothesis that the viscoelasticity of suspensions of these *SBPMG* depends strongly on ϕ_{eff} and the elasticity of the discrete microgel particles (G'_{MG}), which is easily controlled by C_{GEL} (and therefore the crosslinking density). *SBPMGs* therefore represent an important practical analogue for comparison with highly pure, covalently cross-linked synthetic microgels studied and applied elsewhere (e.g. *p(NIPAM)*). Furthermore, the use of natural biopolymers, biocompatible solvents and a facile production technique suggests that covalently cross-linked *SBPMGs* hold promise as functional ingredients for rheology modification (among other applications e.g., encapsulation, stabilization) in formulations where biocompatibility is very important. Varying the ϕ_{eff} of *SBPMG* allows for much higher viscosities to be achieved compared to pectins in their native (*i.e.*, 'non-microgel') state for the same (or lower) overall pectin concentration in the system [21]. Similarly, elasticity can be delivered due to the dense packing of particles rather than polymer chain entanglements as in non-cross-linked *SBP* solutions. This should allow design of desirable flow behavior during processing and during use by the consumer.

CRediT authorship contribution statement

Samuel J. Stubley: Conceptualization, Methodology, Investigation, Formal analysis, Writing – original draft. **Olivier J. Cayre:** Conceptualization, Writing – review & editing, Supervision. **Brent S. Murray:** Conceptualization, Visualization, Writing – review & editing, Supervision, Methodology, Writing – review & editing. **Isabel Celigueta Torres:** Conceptualization.

Declaration of Competing Interest

The authors declare that they have no known competing financial interests or personal relationships that could have appeared to influence the work reported in this paper.

Acknowledgements

We acknowledge and thank Dr. Isabel Fernández Farrés for her support and input into this work during her time at Nestlé. SJS gratefully acknowledges the Engineering and Physical Sciences Research Council (EPSRC) funded Centre for Doctoral Training in Soft Matter and Functional Interfaces (SOFI), Grant Ref. No. EP/L015536/1 as well as Nestlé PTC Confectionery (York, UK) for financial support.

Appendix A. Supplementary data

Supplementary data to this article can be found online at https://doi.org/10.1016/j.jcis.2022.07.147.

References

[1] G. Kavanagh, S. Ross-Murphy, Rheological characterisation of polymer gels, Prog. Polym. Sci. 23 (3) (1998) 533–562.
[2] J. Seth, M. Cloitre, R. Bonnecaze, Elastic properties of soft particle pastes, J. Rheol. 50 (3) (2006) 353–376.
[3] D. Vlassopoulos, M. Cloitre, Tunable rheology of dense soft deformable colloids, Curr. Opin. Colloid Interface Sci. 19 (6) (2014) 561–574.
[4] M. Karg, A. Pich, T. Hellweg, T. Hoare, L.A. Lyon, J.J. Crassous, D. Suzuki, R.A. Gumerov, S. Schneider, I.I. Potemkin, W. Richtering, Nanogels and Microgels: From Model Colloids to Applications, Recent Developments, and Future Trends, Langmuir 35 (19) (2019) 6231–6255.
[5] J. Brijitta, P. Schurtenberger, Responsive hydrogel colloids: Structure, interactions, phase behavior, and equilibrium and nonequilibrium transitions of microgel dispersions, Curr. Opin. Colloid Interface Sci. 40 (2019) 87–103.
[6] P.J. Yunker, K. Chen, M.D. Gratale, M.A. Lohr, T. Still, A.G. Yodh, Physics in ordered and disordered colloidal matter composed of poly(N-isopropylacrylamide) microgel particles, Rep. Prog. Phys. 77 (5) (2014) 056601.
[7] P.N. Pusey, E. Zaccarelli, C. Valeriani, E. Sanz, W.C.K. Poon, M.E. Cates, Hard spheres: crystallization and glass formation, Philosophical Transactions of the Royal Society A: Mathematical, Physical and Engineering Sciences 367 (1909) (2009) 4993–5011.
[8] C.P. Royall, W.C.K. Poon, E.R. Weeks, In search of colloidal hard spheres, Soft Matter 9 (1) (2013) 17–27.
[9] I.J. Joye, D.J. McClements, Biopolymer-based nanoparticles and microparticles: Fabrication, characterization, and application, Curr. Opin. Colloid Interface Sci. 19 (5) (2014) 417–427.
[10] T. Farjami, A. Madadlou, Fabrication methods of biopolymeric microgels and microgel-based hydrogels, Food Hydrocolloids 62 (2017) 262–272.
[11] H.M. Shewan, J.R. Stokes, Review of techniques to manufacture micro-hydrogel particles for the food industry and their applications, J. Food Eng. 119 (4) (2013) 781–792.
[12] H. Shewan, G. Yakubov, M. Bonilla, J. Stokes, Viscoelasticity of non-colloidal hydrogel particle suspensions at the liquid–solid transition, Soft Matter 17 (19) (2021) 5073–5083.
[13] H.M. Shewan, J.R. Stokes, Viscosity of soft spherical micro-hydrogel suspensions, J. Colloid Interface Sci. 442 (2015) 75–81.
[14] S. Adams, W.J. Frith, J.R. Stokes, Influence of particle modulus on the rheological properties of agar microgel suspensions, J. Rheol. 48 (6) (2004) 1195–1213.

[15] D. Garrec, B. Guthrie, I. Norton, Kappa carrageenan fluid gel material properties. Part 1: Rheology, Food Hydrocolloids 33 (1) (2013) 151–159.
[16] M. Caggioni, P.T. Spicer, D.L. Blair, S.E. Lindberg, D.A. Weitz, Rheology and microrheology of a microstructured fluid: The gellan gum case, J. Rheol. 51 (5) (2007) 851–865.
[17] I.T. Norton, D.A. Jarvis, T.J. Foster, A molecular model for the formation and properties of fluid gels, Int. J. Biol. Macromol. 26 (4) (1999) 255–261.
[18] O. Torres, N.M. Tena, B. Murray, A. Sarkar, Novel starch based emulsion gels and emulsion microgel particles: Design, structure and rheology, Carbohydr. Polym. 178 (2017) 86–94.
[19] A. Ellis, J.C. Jacquier, Manufacture and characterisation of agarose microparticles, J. Food Eng. 90 (2) (2009) 141–145.
[20] G.I. Saavedra Isusi, H.P. Karbstein, U.S. van der Schaaf, Microgel particle formation: Influence of mechanical properties of pectin-based gels on microgel particle size distribution, Food Hydrocolloids 94 (2019) 105–113.
[21] S. Stubley, O. Cayre, B. Murray, I. Celigueta Torres, I. Fernández Farrés, Enzyme cross-linked pectin microgel particles for use in foods, Food Hydrocolloids 121 (2021) 107045.
[22] B.R. Thakur, R.K. Singh, A.K. Handa, M.A. Rao, Chemistry and uses of pectin — A review, Crit. Rev. Food Sci. Nutr. 37 (1) (1997) 47–73.
[23] T. Ishii, T. Matsunaga, Isolation and characterization of a boron-rhamnogalacturonan-II complex from cell walls of sugar beet pulp, Carbohydr. Res. 284 (1) (1996) 1–9.
[24] C.M.G.C. Renard, M.-J. Crépeau, J.-F. Thibault, Structure of the repeating units in the rhamnogalacturonic backbone of apple, beet and citrus pectins, Carbohydr. Res. 275 (1) (1995) 155–165.
[25] D.N.A. Zaidel, I.S. Chronakis, A.S. Meyer, Enzyme catalyzed oxidative gelation of sugar beet pectin: Kinetics and rheology, Food Hydrocolloids 28 (1) (2012) 130–140.
[26] J.-F. Thibault, C. Garreau, D. Durand, Kinetics and mechanism of the reaction of ammonium persulfate with ferulic acid and sugar-beet pectins, Carbohydr. Res. 163 (1) (1987) 15–27.
[27] M. Bunzel, Chemistry and occurrence of hydroxycinnamate oligomers, Phytochem. Rev. 9 (1) (2010) 47–64.
[28] C. Johannes, A. Majcherczyk, Laccase activity tests and laccase inhibitors, J. Biotechnol. 78 (2) (2000) 193–199.
[29] K. Almdal, J. Dyre, S. Hvidt, O. Kramer, Towards a phenomenological definition of the term 'gel', Polym. Gels Networks 1 (1) (1993) 5–17.
[30] T.G. Mezger, The Rheology Handbook: For Users of Rotational and Oscillatory Rheometers, 4th ed., Vincentz Network, Hanover, Germany, 2014.
[31] C. Du, R.J. Hill, Linear viscoelasticity of weakly cross-linked hydrogels, J. Rheol. 63 (1) (2018) 109–124.
[32] S. Levigne, M.-C. Ralet, J.-F. Thibault, Characterisation of pectins extracted from fresh sugar beet under different conditions using an experimental design, Carbohydr. Polym. 49 (2) (2002) 145–153.
[33] G.A. Morris, M.-C. Ralet, The effect of neutral sugar distribution on the dilute solution conformation of sugar beet pectin, Carbohydr. Polym. 88 (4) (2012) 1488–1491.
[34] A. Omari, R. Tabary, D. Rousseau, F. Leal Calderon, J. Monteil, G. Chauveteau, Soft water-soluble microgel dispersions: Structure and rheology, J. Colloid Interface Sci. 302 (2) (2006) 537–546.
[35] S. Mueller, E.W. Llewellin, H.M. Mader, The rheology of suspensions of solid particles, Proceedings of the Royal Society A: Mathematical, Physical and Engineering Sciences 466 (2116) (2010) 1201–1228.
[36] P.R. Nott, J.F. Brady, Pressure-driven flow of suspensions: simulation and theory, J. Fluid Mech. 275 (1994) 157–199.
[37] H.M. Wyss, T. Franke, E. Mele, D.A. Weitz, Capillary micromechanics: Measuring the elasticity of microscopic soft objects, Soft Matter 6 (18) (2010) 4550–4555.
[38] M. Desse, D. Fraiseau, J. Mitchell, T. Budtova, Individual swollen starch granules under mechanical stress: evidence for deformation and volume loss, Soft Matter 6 (2) (2010) 363–369.
[39] J. Mattsson, H.M. Wyss, A. Fernandez-Nieves, K. Miyazaki, Z. Hu, D.R. Reichman, D.A. Weitz, Soft colloids make strong glasses, Nature 462 (7269) (2009) 83–86.
[40] K. van der Vaart, Y. Rahmani, R. Zargar, Z. Hu, D. Bonn, P. Schall, Rheology of concentrated soft and hard-sphere suspensions, J. Rheol. 57 (4) (2013) 1195–1209.
[41] H. Senff, W. Richtering, Influence of cross-link density on rheological properties of temperature-sensitive microgel suspensions, Colloid Polym. Sci. 278 (9) (2000) 830–840.
[42] H. Barnes, The yield stress—a review or 'παντα ρει'—everything flows?, J Nonnewton. Fluid Mech. 81 (1) (1999) 133–178.
[43] M. Cross, Rheology of non-Newtonian fluids: A new flow equation for pseudoplastic systems, J. Colloid Sci. 20 (5) (1965) 417–437.
[44] B.H. Tan, R.H. Pelton, K.C. Tam, Microstructure and rheological properties of thermo-responsive poly(N-isopropylacrylamide) microgels, Polymer 51 (14) (2010) 3238–3243.
[45] A. Donev, I. Cisse, D. Sachs, V. Evan, S. Frank, R. Connelly, S. Torquato, P. Chaikin, Improving the Density of Jammed Disordered Packings Using Ellipsoids, Science 303 (5660) (2004) 990–993.
[46] J.S. Chong, E.B. Christiansen, A.D. Baer, Rheology of concentrated suspensions, J. Appl. Polym. Sci. 15 (8) (1971) 2007–2021.
[47] M. Cloitre, R. Borrega, F. Monti, L. Leibler, Structure and flow of polyelectrolyte microgels: from suspensions to glasses, C.R. Phys. 4 (2) (2003) 221–230.
[48] F. Scheffold, P. Díaz-Leyva, M. Reufer, N. Ben Braham, I. Lynch, J. Harden, Brushlike Interactions between Thermoresponsive Microgel Particles, Phys. Rev. Lett. 104 (12) (2010) 128304.
[49] V. Carrier, G. Petekidis, Nonlinear rheology of colloidal glasses of soft thermosensitive microgel particles, J. Rheol. 53 (2) (2009) 245–273.
[50] I. Krieger, T. Dougherty, A Mechanism for Non-Newtonian Flow in Suspensions of Rigid Spheres, Transactions of the Society of Rheology 3 (1) (1959) 137–152.
[51] M.S. Wolfe, C. Scopazzi, Rheology of swellable microgel dispersions: Influence of crosslink density, J. Colloid Interface Sci. 133 (1) (1989) 265–277.
[52] N. Koumakis, G. Petekidis, Two step yielding in attractive colloids: transition from gels to attractive glasses, Soft Matter 7 (6) (2011) 2456–2470.
[53] M. Laurati, S.U. Egelhaaf, G. Petekidis, Nonlinear rheology of colloidal gels with intermediate volume fraction, J. Rheol. 55 (3) (2011) 673–706.
[54] N. Koumakis, A. Pamvouxoglou, A.S. Poulos, G. Petekidis, Direct comparison of the rheology of model hard and soft particle glasses, Soft Matter 8 (15) (2012) 4271–4284.
[55] T.G. Mason, M. Lacasse, G. Grest, D. Levine, J. Bibette, D.A. Weitz, Osmotic pressure and viscoelastic shear moduli of concentrated emulsions, Phys. Rev. E 56 (3) (1997) 3150–3166.
[56] M. Siebenbürger, M. Fuchs, H. Winter, M. Ballauff, Viscoelasticity and shear flow of concentrated, noncrystallizing colloidal suspensions: Comparison with mode-coupling theory, J. Rheol. 53 (3) (2009) 707–726.
[57] J.J. Crassous, M. Siebenbürger, M. Ballauff, M. Drechsler, D. Hajnal, O. Henrich, M. Fuchs, Shear stresses of colloidal dispersions at the glass transition in equilibrium and in flow, J. Chem. Phys. 128 (20) (2008) 204902.
[58] M. Helgeson, N. Wagner, D. Vlassopoulos, Viscoelasticity and shear melting of colloidal star polymer glasses, J. Rheol. 51 (2) (2007) 297–316.
[59] S.E. Paulin, B.J. Ackerson, M.S. Wolfe, Equilibrium and Shear Induced Nonequilibrium Phase Behavior of PMMA Microgel Spheres, J. Colloid Interface Sci. 178 (1) (1996) 251–262.
[60] J. Yang, K. Schweizer, Tunable dynamic fragility and elasticity in dense suspensions of many-arm-star polymer colloids, EPL (Europhysics Letters) 90 (6) (2010) 66001.
[61] D.M. Heyes, A.C. Brańka, Interactions between microgel particles, Soft Matter 5 (14) (2009) 2681–2685.
[62] I. Evans, A. Lips, Concentration dependence of the linear elastic behaviour of model microgel dispersions, J. Chem. Soc., Faraday Trans. 86 (20) (1990) 3413–3417.
[63] S.H. Ching, N. Bansal, B. Bhandari, Rheology of emulsion-filled alginate microgel suspensions, Food Res. Int. 80 (2016) 50–60.
[64] G. Petekidis, A. Moussaïd, P.N. Pusey, Rearrangements in hard-sphere glasses under oscillatory shear strain, Phys. Rev. E 66 (5) (2002) 051402.
[65] K.N. Pham, G. Petekidis, D. Vlassopoulos, S.U. Egelhaaf, P.N. Pusey, W.C.K. Poon, Yielding of colloidal glasses, Europhysics Letters (EPL) 75 (4) (2006) 624–630.
[66] A. Le Grand, G. Petekidis, Effects of particle softness on the rheology and yielding of colloidal glasses, Rheol. Acta 47 (5) (2008) 579–590.
[67] R.J. Ketz, R.K. Prud'homme, W.W. Graessley, Rheology of concentrated microgel solutions, Rheol. Acta 27 (5) (1988) 531–539.
[68] N. Koumakis, A.B. Schofield, G. Petekidis, Effects of shear induced crystallization on the rheology and ageing of hard sphere glasses, Soft Matter 4 (10) (2008) 2008–2018.